Research Article

Nano Biomed Eng

Different Approaches for Silver Nanoparticle Sterilization for Administration to Cell Culture

Aleksandra Zimon[1,2], Agnieszka M. Kołodziejczyk[1,2], Magdalena M. Grala[1,2], Piotr Komorowski[1,2,3]

[1] Nanomaterial Structural Research Laboratory, Bionanopark Ltd., Lodz, Poland
[2] Molecular and Nanostructural Biophysics Laboratory, Bionanopark Ltd., Lodz, Poland
[3] Department of Biophysics, Institute of Materials Science and Engineering, Lodz University of Technology, Lodz, Poland

Corresponding author. E-mail: aga.szczygiel@gmail.com

Received: Mar. 2, 2022; **Revised:** Jan. 30, 2023; **Accepted:** May 17, 2023

Citation: A. Zimon, A.M. Kołodziejczyk, M.M. Grala, et al. Different approaches for silver nanoparticle sterilization for administration to cell culture. *Nano Biomedicine and Engineering*, 2023, 15(3): 253−261.

http://doi.org/10.26599/NBE.2023.9290019

Abstract

In recent years, there has been increased interest in the use of nanostructures in various industries, such as the food, textile, pharmaceutical, electronics, and chemical industries. Most of these applications require a proper preparation of specific nanomaterials. In this study, we characterized silver nanoparticles (AgNPs) stabilized with polyvinylpyrrolidone and prepared in aqueous suspensions using dynamic light scattering, atomic force microscopy, and transmission electron microscopy. We aimed to compare the influence of different AgNP preparation procedures, specifically autoclaving, sonication, and a combination of both, on the agglomeration of these nanoparticles. Additionally, the toxicity of the NPs after the selected sterilization methods toward the EA.hy926 endothelial cell line was determined using trypan blue labeling, 2,3-bis-(2-methoxy-4-nitro-5-sulfophenyl)-2H-tetrazolium-5-carboxanilide (XTT) tetrazolium salt reduction tests, and the 3-[4,5-dimethylthiazol-2yl]-2,5-diphenyltetrazolium bromide (MTT) tetrazolium bromide test. Based on the obtained results, we concluded that cells exposed to AgNPs after sonication had similar viability values above 80% across all cellular viability tests. Conversely, the cellular viability values of the EA.hy926 cell line exposed to the autoclaved AgNP solutions differed. From the XTT tests, we observed a falsely determined cellular viability value above 100% with a simultaneous increase in the XTT-measured absorbance for the cellular medium after autoclaving. However, the other viability tests showed a cellular viability value below 25%. The results prove the importance of selecting an appropriate method for measuring cell viability, especially for cells exposed to previously sterilized nanomaterials.

Keywords: silver nanoparticles (AgNPs); sonication; autoclaving; cellular viability; 2,3-bis-(2-methoxy-4-nitro-5-sulfophenyl)-2H-tetrazolium-5-carboxanilide (XTT); 3-[4,5-dimethylthiazol-2yl]-2,5-diphenyltetrazolium bromide (MTT)

Introduction

Recently, nanomaterials have been tested for use in the food, pharmaceutical, textile, electronics, and automotive industries as gas sensors, optical devices, water purification devices, and pollution-monitoring sensors. Nanomaterials also have applications as antibacterial agents and functional nanocomposites, as well as in cosmetology, sports and recreation, membrane and filter production, and food packaging.

A critical aspect of nanomaterial application is in biomedical sciences, particularly oncology, pharmacy, and the development of implants and drug carriers for targeted therapy (i.e., drug delivery to affected areas without interfering with healthy tissues) [1]. Due to the wide range of applications and potential of nanomaterials, the preparation of nanostructures for administration in cell cultures should be carefully analyzed. Conducting *in vitro* studies is a key step in identifying the toxic effects of nanostructures on cells or confirming their absence. However, preparing nanostructures involves several challenges regarding the preparation of a stable solution in an aqueous suspension that closely resembles the cellular medium [2]. Thus, processes such as presterilizing the suspension, reducing agglomerate formation, and selecting the appropriate concentration must be considered [3–5]. Understanding the effects of nanostructures on cells, including agglomeration after administration to cell culture [6, 7], nanoparticle (NP) endocytosis by cells, and their potential toxic effects, is crucial. Many research groups are currently investigating the cell–nanomaterial interaction to determine when cells undergo harmless adaptive changes and the point at which their defensive reaction to the stress caused by the presence of nanomaterials in their environment is initiated [8–10]. One of the extensively studied NPs in the literature is silver nanoparticles (AgNPs). AgNPs can trigger many undesirable processes in cells, including elevated levels of reactive oxygen species, polymerization of actin fibers, cell stiffening, andeventheinitiationofprocessesinducingapoptosis[11]. The effect of AgNPs on EA.hy926 cells differs between low and high passages [12, 13].

In this study, we present various methods of preparing AgNPs that can be used in studying cell cultures. Furthermore, the effects of the selected sterilization methods, such as autoclaving and sonication, are presented for the first time. These sterilization methods are among the cheapest and most available methods of preparing materials in biological laboratories. Many biological substances and reagents used in cell culture to maintain the appropriate quality level undergo autoclaving. These include water, phosphate buffers, and Hanks' buffers. Conversely, the sonication method facilitates the improved preparation of AgNPs by simultaneously breaking up agglomerates or aggregates and sterilizing the colloid before its administration to the cell culture. Note that AgNP suspensions were sonicated or autoclaved in the multicomponent cellular medium. However, cell culture can be conducted under appropriate conditions in a complete supplemented medium, which closely mimics the physiological state of the cells. After the sterilization processes, AgNPs were examined using transmission electron microscopy (TEM) and dynamic light scattering (DLS) and presented the effect of filtering the AgNP suspension using atomic force microscopy (AFM). Additionally, we investigated the influence of AgNPs on EA.hy926 cell viability. Cellular viability was assessed using 2,3-bis-(2-methoxy-4-nitro-5-sulfophenyl)-2H-tetrazolium-5-carboxanilide (XTT) tetrazolium salt reduction tests, the 3-[4,5-dimethylthiazol-2-yl]-2,5-diphenyltetrazolium bromide (MTT) tetrazolium bromide test, and trypan blue labeling. Among colorimetric methods, MTT and XTT cell viability assays are extensively used in the cytotoxicity screening of drugs, chemical compounds, physical agents, biomaterials, nanotechnology products, and other substances that can affect cell health or cell metabolism. Both assays are rapid, cheap, reproducible, and available for routine toxicity screening. Unfortunately, many factors can influence MTT and XTT reduction performances. To explain the differences in cellular viability, we conducted XTT tests on a conditioned cellular medium without cells.

Experimental

AgNP nanopowder stabilized with polyvinyl pyrrolidone was purchased from Sigma-Aldrich (Cat. 576832, Saint Louis, USA). The AgNP suspensions in 1 mg/mL demineralized water were initially subjected to autoclaving (121 °C) and/or sonication (ultrasound generator power of 128 W). Immediately after the selected sterilization methods, the AgNP suspensions were deposited onto TEM grids comprising a Cu 300 mesh with a carbon film. Simultaneously, the sonicated AgNP suspensions were filtered using a 0.2 μm pore size filter, placed on a cleaved mica surface, and left to dry at room temperature for AFM measurements. Unfiltered AgNP solutions were deposited on the mica for comparison.

TEM and AFM

TEM imaging was performed using a Talos F200X microscope (FEI, The Netherlands) at an acceleration voltage of 200 kV. AFM was performed on a Bioscope Resolve microscope (Bruker, USA) using Peak Force Tapping mode in an air environment. Measurements were conducted using a Scan Asyst Air probe (Bruker, USA) with 0.4 N/m spring constant cantilevers.

Dynamic light scattering

The hydrodynamic radius distribution of the AgNP suspensions after the selected sterilization methods (autoclaving, sonication, autoclaving followed by sonication, sonication followed by filtering) was measured using DLS. Immediately after preparation, 20 µL of AgNP solutions were placed in a disposable cuvette. Five measurements of 10 acquisitions each were collected at 25 °C. Regularization analysis was employed to calculate the hydrodynamic radius (R) of AgNPs [14].

Cell culture

The studies were conducted on the EA.hy926 endothelial cell line (ATCC-CRL-2922, USA). Cells were cultured in Dulbecco's Modified Eagle Medium (DMEM, ATCC, Virginia, USA), supplemented with fetal bovine serum (Gibco) and penicillin/streptomycin cocktail (ATCC, Virginia, USA), and maintained at 37°C in a humidified atmosphere of 9% CO_2. The details of the cell culture protocol are described in a previous study [11]. The EA.hy926 cells were passaged every 2 to 3 d when they reached a 90% to 100% confluence on the culture dishes. To detach the cells from the culture dish, they were first rinsed with Dulbecco's phosphate-buffered saline (ATCC, Virginia, USA), trypsinized from the culture dishes using Trypsin-EDTA (ATCC, Virginia, USA) for 3 min, and then neutralized in a 10-fold volume of complete DMEM. Subsequently, the cells were centrifuged for 5 min at 800 r/min and seeded at the desired density on proper dishes for the selected measurements.

Cytotoxicity tests using XTT and MTT assays and trypan blue labeling

The EA.hy926 cells were seeded onto 96-well plates at a density of 1×10^4 cells per well and incubated for 24 h. Subsequently, the cells were exposed to AgNPs at a concentration of 10 µg/mL for 24 h using the selected sterilization methods (autoclaving and sonication) for XTT and MTT tests. Six replicates (one column of the 96-well plates) were prepared for each sample, and the measurements were collected for three different passages of EA.hy926 cells.

For XTT measurements, XTT reagent (Biological Industries, Cromwell, USA) was added to the cells following the manufacturer's protocol. Briefly, 50 µL of the XTT mixture solution (buffer reagent and activator) was added to each well of the 96-well plates, and the reduction reaction occurred at 37 °C for 4 h under sterile conditions. Next, 100 µL of supernatants supplemented with XTT reagent were collected into a 96-well plate. The absorbance of the orange-colored formazan product was measured using a Victor X4 microplate reader (Perkin Elmer, USA) at a wavelength of 450 nm. XTT tests were conducted for the conditioned (9% CO_2 at 37 °C) DMEM after autoclaving, AgNPs suspended in DMEM and sterilized using the selected sterilization methods, and AgNPs suspended in Milli-Q (mQ) water. The XTT measurement values for the media and AgNP suspensions were presented as the mean absorbance values.

For MTT measurements, the cell supernatants were removed from the 96-well plates. Next, MTT salt (Sigma-Aldrich, Saint Louis, USA) with a concentration of 1 mg/mL was added to the cell culture and incubated for 4 h. After incubating the cells with the MTT reagent, the solution was removed from the cells, and an appropriate amount of a solution of 0.04 mmol/L hydrochloric acid in 70% isopropanol was added for the complete dissolution of formazan crystals. The absorbance of the formed formazan compounds was measured using a Victor X4 microplate reader at a wavelength of 570 nm.

Cell viability for the XTT and MTT measurements was calculated as follows:

$$\text{Viability} = (A/A_C) \times 100\%$$

where A is the absorbance of an investigated sample, and A_C is the absorbance of the control (untreated cells). The mean and SD values were calculated for each experimental point.

Furthermore, a trypan blue (Cheminst, Poland) labeling test was conducted. In this case, EA.hy926 cells were seeded onto 12-well plates at a density of 5×10^4 cells per well and incubated for 24 h, followed by incubation with AgNPs for 24 h. Next, cells were

passaged as described in the cell culture section. The cell pellets from each well of the plate were suspended in 200 μL of fresh culture medium and labeled with trypan blue in a ratio of 1:1. Afterward, cells were collected using an EVE™ automatic cell counter (NanoEnTek, Seoul, Republic of Korea). The test was conducted in triplicate, and the mean and standard deviation (SD) values of cell viability were expressed as a percentage of the control (untreated cells).

For light microscopy (bright field) observations, seeded cells were cultured onto 12-well plates, followed by AgNP treatment, consistent with the trypan blue labeling process. The EA.hy926 cells were visualized using an IX73 Olympus (Olympus, Japan) microscope (10× objective) with CellSense (Olympus, Japan) software. At least five images were collected for one experimental point.

Results

Figure 1 shows the distributions of scattered light intensity as a function of the hydrodynamic radius of AgNPs after autoclaving (Fig. 1(a)), after autoclaving and sonication (Fig. 1(b)), after only sonication (Fig. 1(c)), and after sonication and filtration (Fig. 1(d)). Additionally, the mean values of the radius, percentage of polydispersity, and percentage of mass (insets of tables in Fig. 1) were determined.

The AgNP suspensions in demineralized water after sonication, autoclaving, and a combination of both preparation methods were deposited on Cu mesh grids and visualized using TEM (Fig. 2).

Figure 3 shows the comparative results of AFM for AgNPs deposited on the mica after sonication (Figs. 3(a) and 3(b)) and after sonication and filtering (Figs. 3(c)–3(f)). Figures 3(a) and 3(b) show several large AgNP agglomerates on the sample surface. We removed large agglomerates using filtration (Figs. 3(c)–3(f)), which enabled the imaging of single NPs.

Figure 4(a) shows the mean absorbance value of XTT tests for DMEM and AgNPs prepared in DMEM and mQ water after the selected sterilization processes, including autoclaving and sonication. Figure 4(b) shows the cellular viability comparison of cells exposed to AgNPs at a 10 μg/mL concentration using different preparation procedures for XTT, MTT, and trypan blue labeling tests. Figure 4(c) presents the optical microscopy images of endothelial cells. Unexpectedly, the AgNPs that were suspended in the medium and then autoclaved, as well as the medium itself after autoclaving, showed a false increase in absorbance. Note that for the medium and the AgNP suspensions, there should be no increase in absorbance in XTT measurements. Cellular media or

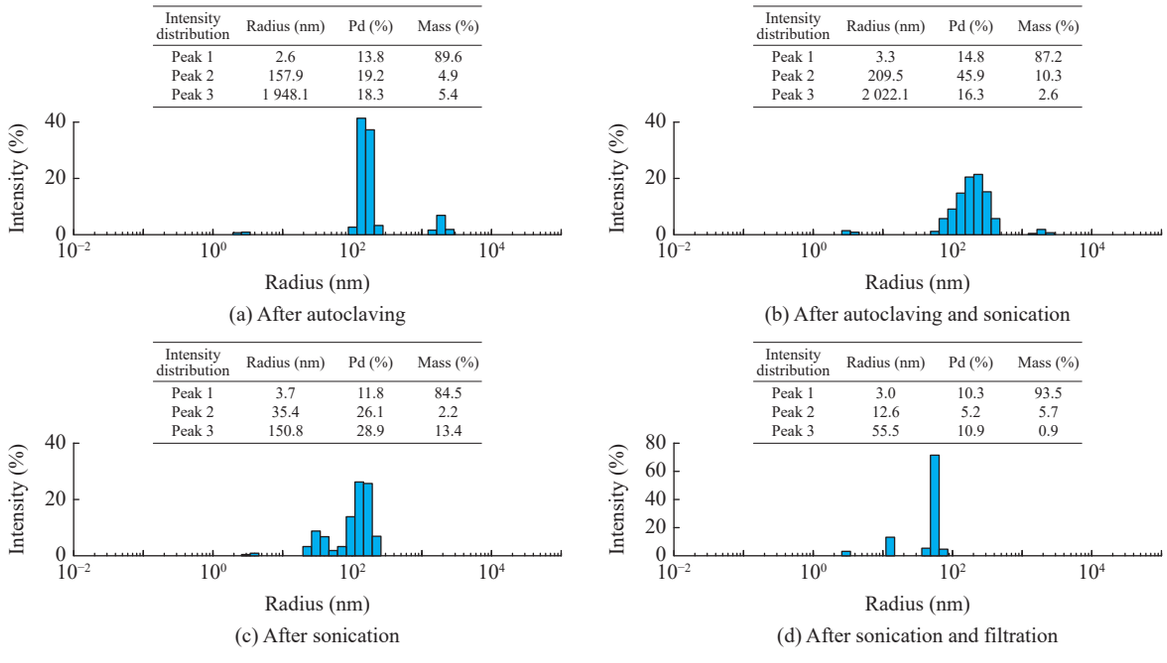

Fig. 1 The hydrodynamic radius distributions of AgNPs suspended in demineralized water at a concentration of 1 mg/mL **(a)** after autoclaving, **(b)** after autoclaving and sonication, **(c)** after sonication, and **(d)** after sonication and filtration. The insets present the mean values of radiuses for each detected peak, the percentage of polydispersity, and the percentage of mass.

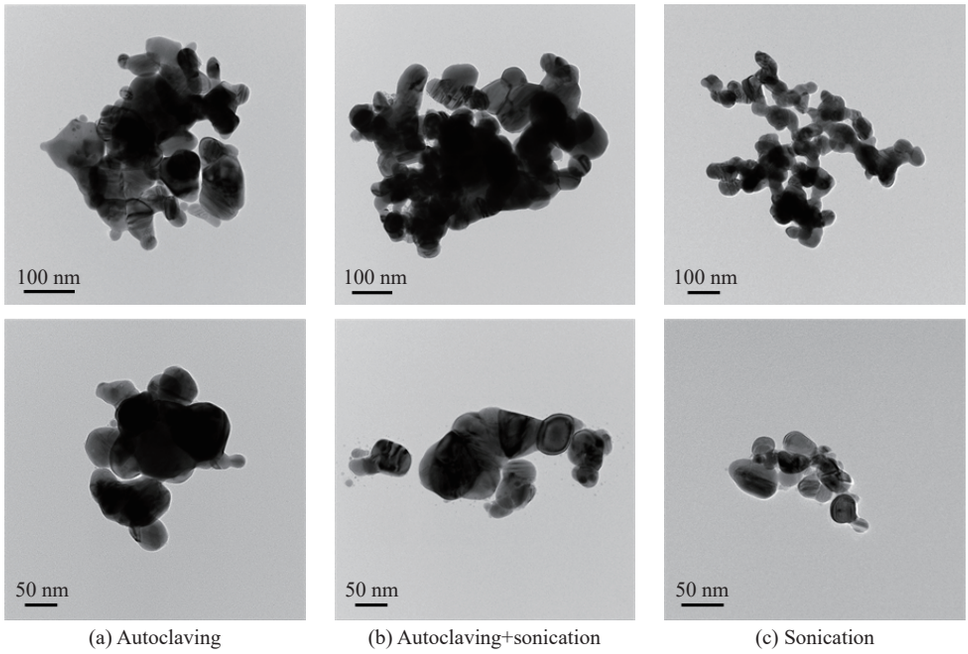

Fig. 2 TEM images of AgNPs **(a)** after autoclaving, **(b)** after autoclaving and sonication, and **(c)** after sonication. Bottom images present AgNPs at the maximum magnification.

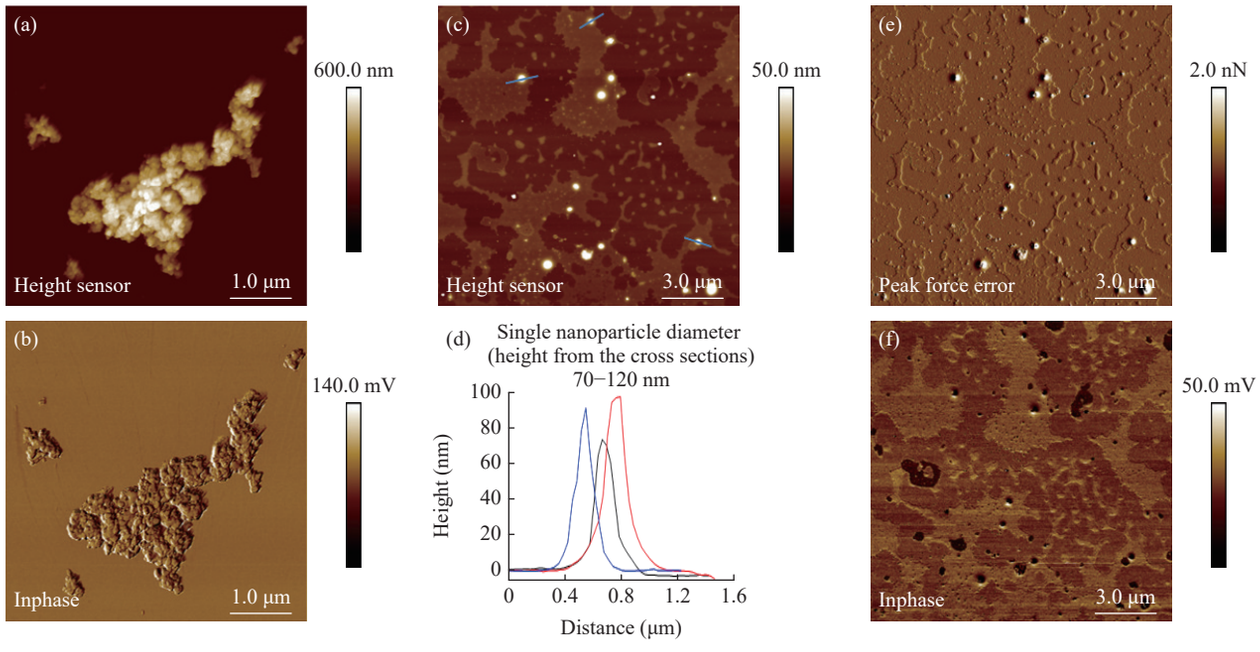

Fig. 3 AFM images of the **(a)** surface topography **(b)** and inphase of AgNPs after sonication, as well as **(c)** surface topography, **(d)** cross-section profiles, **(e)** peak force error, and **(f)** inphase of AgNPs after sonication and filtration

AgNP suspensions administered to cell cultures are defined as "blank" for this type of measurement. This result suggests a reaction of the XTT reagent with the medium after autoclaving, which may be related to the thermal decomposition of the compounds from the cellular medium, as described in the Discussion section. The absorbance for AgNPs that were suspended in DMEM and then sonicated is at the same level as that for pure DMEM (Fig. 4(a), gray bars). Untreated cells were defined as a control for each experiment (Fig. 4(b), control), and they have the same cell viability values for selected methods.

EA.hy926 cells exposed to 10 µg/mL of AgNPs after sonication revealed similar cell viability values (about 83%) for the XTT, MTT, and trypan blue labeling tests (Fig. 4(b), AgNP-S). The XTT tests conducted for cells exposed to sonicated AgNPs did not show a false increase in absorbance.

High differences in cell viability for the three tests

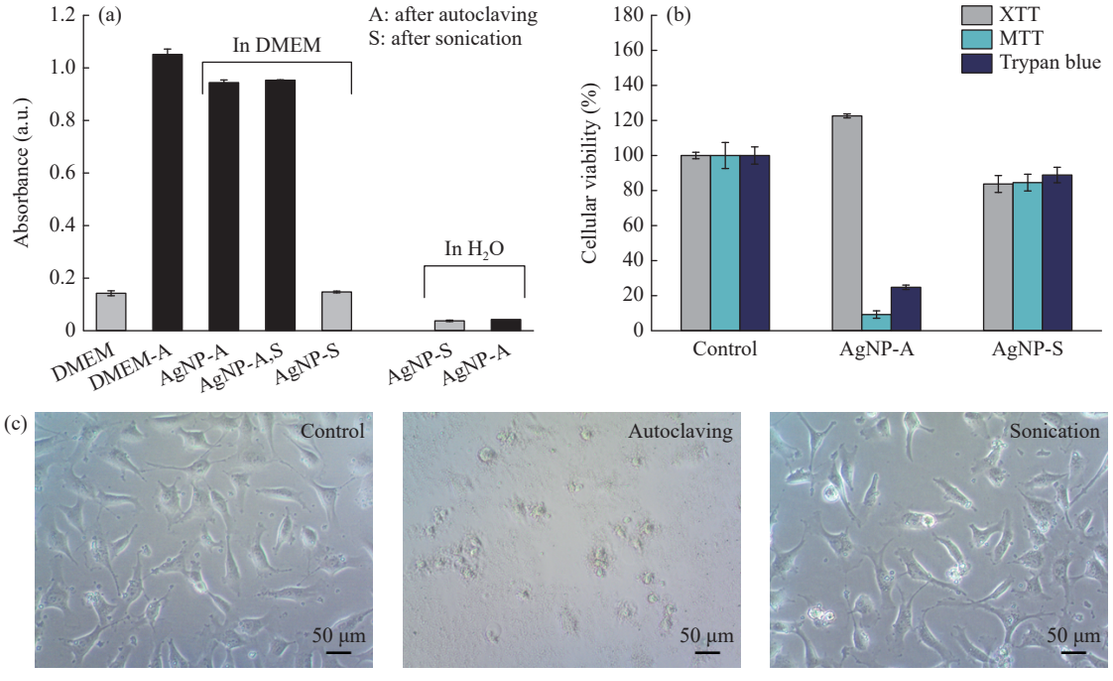

Fig. 4 (a) XTT measurements obtained for DMEM and AgNPs after the selected preparation procedures; **(b)** the cellular viability of EA.hy926 cells exposed to AgNPs after autoclaving and sonication in DMEM, measured using XTT, MTT, and trypan blue labeling; and **(c)** light microscopy images of EA.hy926 cells exposed to AgNPs. Autoclaving and sonication were marked as A and S, respectively. Black bars correspond to the mean absorbance values of autoclaved media (DMEM-A), including autoclaved AgNP suspensions (AgNP-A, AgNP-A,S) after XTT reduction tests. Gray bars indicate the mean absorbance values from the XTT test of the pure medium (DMEM), sonicated AgNP suspensions prepared in DMEM (AgNP-S in DMEM), and sonicated AgNP suspensions prepared in water (AgNP-S in H_2O).

were obtained for EA.hy926 cells exposed to autoclaved AgNP suspensions (Fig. 4(b), AgNP-A). The values of the MTT and trypan blue labeling tests are from 10% to 20%, corresponding to the cell morphology observed on the light microscopy images (Fig. 4(c), autoclaving). The increase in cell viability value observed in the XTT tests is due to the false increase in the absorbance of autoclaved AgNP suspensions (Fig. 4(a)).

Discussion

The sterilization processes of NP suspensions to be administered to cell cultures are a primary issue that requires careful examination. AgNPs are often available as powders. Thus, preparing AgNP suspensions is important regarding their stability and sterilization processes. However, filtration sterilization should be omitted, as it could change the NP concentration. Filtration can be used to remove NP agglomerates and thus verify the presence of a smaller NP population. Filtered and unfiltered AgNPs on the mica were imaged using AFM. The cross-sections of filtered AgNPs (Fig. 3(d)) showed that the diameters of single NPs ranged from 70 to 120 nm. Considering the biological influence of AgNPs on cells, it is important to confirm the presence of smaller NPs.

The incubation of cells with AgNPs was conducted in a cellular medium in a physiological environment. Due to the 24-h cell exposure to AgNPs, silver agglomerates were observed on the membrane surface and in the cellular interior, which was published in our previous works [11–13]. The agglomeration processes of AgNPs may be influenced by other factors in the cellular medium (e.g., antibiotics, L-glutamine, and glucose), through which we maintain static cell culture under physiological conditions. Thus, AgNP sterilization, which prevents the formation of nanomaterial agglomerates and aggregates, is crucial for administration to cell culture. The size of AgNPs [15–17] or their agglomerates [18, 19] may have a different effect on cells, that is, on the interaction of NPs with lipid proteins and thus initiate intracellular processes at the molecular level.

The AgNP sterilization procedures discussed in this study include autoclaving, sonication, and a combination of both. The characterization of AgNPs after performing the selected sterilization procedures

was conducted using DLS and TEM. Independent of the preparation method, we observed a population of small NPs and/or a stabilizer with a radius of 2.6–3.7 nm for all cases measured using DLS. From the comparison of DLS histograms in Figs. 1(a) and 1(b), we can conclude that autoclaving of AgNP suspensions may induce the formation of agglomerates that cannot be separated through sonication. After sonication (Fig. 1(c)), a population of AgNPs with a radius of 35 nm was obtained, indicating an improved separation of larger agglomerates. The filtration process eliminates large agglomerates; therefore, smaller NPs, including those with a radius of 11 nm, are detectable (Fig. 1(d)). DLS measurements reflect the "state of the samples" fed into the cell culture more closely than TEM and quantify the differences between AgNP colloids after the selected sterilization procedures. Conversely, TEM was conducted for samples placed on the Cu 300 mesh with carbon film grids and left to dry at room temperature. Drying of the sample can cause increased agglomeration (i.e., single AgNPs connecting to larger clusters). From the TEM images, we can confirm the formation of large AgNP aggregates (Fig. 2(a)) after autoclaving processes. Sonication can be used to break up AgNP aggregates (Fig. 2(c)), but this process is strongly limited after autoclaving (Fig. 2(b)).

Colorimetric methods for measuring cell viability are based on the observation that tetrazolium salts, as electron acceptors, are converted by living cells to colored formazan compounds. MTT is a positively charged compound that easily enters the cell, where it is reduced to water-insoluble formazan [20]. The formazan crystals formed after the reduction should be dissolved in an organic solvent. Conversely, XTT salt is converted into an aqueous soluble product [21]. Due to their negative charge, XTT and other second-generation tetrazolium salts penetrate poorly into the cells. Therefore, the reduction process occurs mainly on the cell surface or in the plasma membrane, with the participation of the transmembrane electron transport chain [22]. Tests based on MTT and XTT reduction are increasingly used in laboratory practice [22] to determine the sensitivity of microorganisms to drugs [23], measure viability [24, 25], or assess the proliferation intensity of eukaryotic cells in response to cytokines [26], nanostructures [27], or drugs. The physicochemical properties of tetrazolium salts determine the different locations of their reduction process (mitochondria, cytosol, and outer membrane) and the varied participation of cellular reductants in their conversion. The application of XTT and MTT tests to a specific research task should be preceded by a preliminary study aimed at optimizing the experiment conditions. In this study, we aimed to determine whether XTT and MTT salts interact (reduce) with the cellular medium in which AgNPs are administered to the cell culture.

XTT tests performed on cells exposed to autoclaved AgNPs achieved a much higher cell viability than for control cells and for MTT and trypan blue labeling tests). Cell viability was about 10% for the MTT test and about 25% for trypan blue labeling. To determine whether the XTT tests correctly determined cell viability in the autoclaved medium, we conducted XTT tests for the autoclaved medium and for AgNPs that were suspended in DMEM and then autoclaved (Fig. 4(a)) without contact with cells. An increase in absorbance was obtained for both cases. In addition, no increase in absorbance was obtained for AgNPs that were suspended in water and then autoclaved. The false XTT result was related to the false-positive XTT test for autoclaving the cell culture medium containing L-glutamine. A previous study [28] reported that the complete decomposition of a 2 mmol/L L-glutamine solution occurred within 30 min at 121 °C. This thermal decomposition of L-glutamine influences AgNP colloids and cell viability values for XTT, MTT, and trypan blue labeling measurements. The data on the thermal decomposition of aqueous solutions of L-glutamine indicate its unsuitability as an autoclavable substrate and emphasize the necessity of filtration sterilization. However, as previously discussed, filtration sterilization cannot be used to prepare a nanostructure suspension in a cellular medium.

Sonication is one of the methods that can be used to sterilize AgNP suspensions. According to the literature, the sonication procedure exhibited a significant time-dependent antibacterial effect [29] and could be used for nonthermal disinfection processes [30]. In this study, the sonicated AgNP suspensions were administered to an endothelial cell culture to determine the appropriate cytotoxicity tests. The viability (83%) of EA.hy926 cells exposed to sonicated AgNPs was lower than that for the control sample (untreated cells). This cellular viability value

was confirmed through MTT, XTT, and trypan blue labeling tests (Fig. 4(b)). Note that the XTT tests performed for sonicated AgNPs did not show a false increase in absorbance. From the optical images, the obtained cell viability results correspond with the distinct morphology changes in cells exposed to autoclaved or sonicated AgNPs (Fig. 4(c)). The toxicity of AgNPs depends on the cell line and cell culture conditions, including whether the tests were conducted in a complete cellular medium with fetal bovine serum. In our previous studies [11–13], we conducted tests on EA.hy926 cells exposed to AgNPs in a serum-free cell culture medium, and we observed a decrease in cell viability to about 60% for a concentration of 10 μg/mL [12]. In this study, the tests were conducted in a fetal-bovine-serum-supplemented medium, and the cell viability was above 80%. Thus, we can conclude that a serum masks and delays the effect of AgNPs.

Conclusion

The autoclaving process can induce the formation of AgNP agglomerates. Conversely, the sonication method mostly disintegrates NP aggregates but becomes less efficient after autoclaving. The hydrodynamic radius distribution of AgNPs obtained from DLS measurements confirms the occurrence of aggregation in the autoclaved suspensions.

Our result shows the limitation of XTT tests in cell viability measurements with AgNPs in a cellular medium containing L-glutamine. The same values of cellular viability were obtained across the selected viability tests (XTT, MTT, and trypan blue labeling) for EA.hy926 cells that were exposed to AgNPs and then sonicated. This result may confirm the importance of selecting an appropriate measurement method for cell viability. In determining the cytotoxicity assay method, it is important to choose an appropriate method that can measure the toxicity of interest without a false-negative or false-positive misinterpretation of the toxicity result.

CRediT Author Statement

Aleksandra Zimon: Data curation, Writing–review and editing, Methodology, Conceptualization, Investigation, Writing–review & editing, Supervision. **Agnieszka M. Kołodziejczyk**: Conceptualization, Investigation, Project administration, Visualization, Writing – original draft, Writing–review & editing. **Magdalena M. Grala**: Data curation, Formal analysis, Investigation, Writing – original draft. **Piotr Komorowski:** Funding acquisition, Visualization.

Acknowledgement

This work is financed by The National Science Centre, project title: “The influence of selected nanoparticles on the elastic properties of endothelial cells evaluated using atomic force microscopy”, agreement No. 2017/26/D/ST4/00918.

Conflict of Interest

The authors declare that no competing interest exists.

References

[1] A.M. Grumezescu. Nanostructures for the engineering of cells, tissues and organs: From design to applications. Elsevier, 2018. https://doi.org/10.1016/C2016-0-04102-5

[2] N. Baig, I. Kammakakam, W. Falath. Nanomaterials: A review of synthesis methods, properties, recent progress, and challenges. *Materials Advances*, 2021, 2(6): 1821−1871. https://doi.org/10.1039/D0MA00807A

[3] S. Dutz, S. Wojahn, C. Gräfe, et al. Influence of sterilization and preservation procedures on the integrity of serum protein-coated magnetic nanoparticles. *Nanomaterials*, 2017, 7(12): 453. https://doi.org/10.3390/nano7120453

[4] J.W. Zheng, J.D. Clogston, A.K. Patri, et al. Sterilization of silver nanoparticles using standard gamma irradiation procedure affects particle integrity and biocompatibility. *Journal of Nanomedicine & Nanotechnology*, 2011, 2011(Suppl 5): 001. https://doi.org/10.4172/2157-7439.S5-001

[5] H. Rokbani, F. Daigle, A. Ajji. Combined effect of ultrasound stimulations and autoclaving on the enhancement of antibacterial activity of ZnO and SiO_2/ZnO nanoparticles. *Nanomaterials*, 2018, 8(3): 129. https://doi.org/10.3390/nano8030129

[6] S. Murugadoss, S. Mülhopt, S. Diabaté, et al. Agglomeration state of titanium-dioxide (TiO_2) nanomaterials influences the dose deposition and cytotoxic responses in human bronchial epithelial cells at the air-liquid interface. *Nanomaterials*, 2021, 11(12): 3226. https://doi.org/10.3390/nano11123226

[7] B. Halamoda-Kenzaoui, M. Ceridono, P. Urbán, et al. The agglomeration state of nanoparticles can influence the mechanism of their cellular internalisation. *Journal of Nanobiotechnology*, 2017, 15(1): 48. https://doi.org/10.1186/s12951-017-0281-6

[8] C. Auría-Soro, T. Nesma, P. Juanes-Velasco, et al. Interactions of nanoparticles and biosystems: Microenvironment of nanoparticles and biomolecules in nanomedicine. *Nanomaterials*, 2019, 9(10): 1365. https://doi.org/10.3390/nano9101365

[9] Q.Q. Huang, J.C. Zhang, Y.Y. Zhang, et al. Adaptive changes induced by noble-metal nanostructures *in vitro* and *in vivo*. *Theranostics*, 2020, 10(13): 5649–5670. https://www.thno.org/v10p5649.htm

[10] M. Bundschuh, J. Filser, S. Lüderwald, et al. Nanoparticles in the environment: Where do we come from, where do we go to. *Environmental Sciences Europe*, 2018, 30(1): 6. https://doi.org/10.1186/s12302-018-0132-6

[11] A.M. Kolodziejczyk, P. Sokolowska, A. Zimon, et al. Dysfunction of endothelial cells exposed to nanomaterials assessed by atomic force spectroscopy. *Micron*, 2021, 145: 103062. https://doi.org/10.1016/j.micron.2021.103062

[12] A.M. Kolodziejczyk, A. Jakubowska, M. Kucinska, et al. Sensing of silver nanoparticles on/in endothelial cells using atomic force spectroscopy. *Journal of Molecular Recognition*, 2018, 31(9): e2723. https://doi.org/10.1002/jmr.2723

[13] A.M. Kolodziejczyk, M. Kucinska, A. Jakubowska, et al. Endothelial cell aging detection by means of atomic force spectroscopy. *Journal of Molecular Recognition*, 2020, 33(12): e2853. https://doi.org/10.1002/jmr.2853

[14] J. Stetefeld, S.A. McKenna, T.R. Patel. Dynamic light scattering: A practical guide and applications in biomedical sciences. *Biophysical Reviews*, 2016, 8(4): 409–427. https://doi.org/10.1007/s12551-016-0218-6

[15] K. Kettler, P. Krystek, C. Giannakou, et al. Exploring the effect of silver nanoparticle size and medium composition on uptake into pulmonary epithelial 16HBE14o-cells. *Journal of Nanoparticle Research*, 2016, 18(7): 182. https://doi.org/10.1007/s11051-016-3493-z

[16] A. Lankoff, W.J. Sandberg, A. Wegierek-Ciuk, et al. The effect of agglomeration state of silver and titanium dioxide nanoparticles on cellular response of HepG2, A549 and THP-1 cells. *Toxicology Letters*, 2012, 208(3): 197–213. https://doi.org/10.1016/j.toxlet.2011.11.006

[17] K.S. Butler, D.J. Peeler, B.J. Casey, et al. Silver nanoparticles: Correlating nanoparticle size and cellular uptake with genotoxicity. *Mutagenesis*, 2015, 30(4): 577–591. https://doi.org/10.1093/mutage/gev020

[18] M.K. Ha, Y.J. Shim, T.H. Yoon. Effects of agglomeration on *in vitro* dosimetry and cellular association of silver nanoparticles. *Environmental Science*: *Nano*, 2018, 5(2): 446–455. https://doi.org/10.1039/C7EN00965H

[19] M.R. Kalbassi, S.A. Johari, M. Soltani, et al. Particle size and agglomeration affect the toxicity levels of silver nanoparticle types in aquatic environment. *ECOPERSIA*, 2013, 1(3): 273–290.

[20] T. Mosmann. Rapid colorimetric assay for cellular growth and survival: Application to proliferation and cytotoxicity assays. *Journal of Immunological Methods*, 1983, 65(1/2): 55–63. https://doi.org/10.1016/0022-1759(83)90303-4

[21] D.A. Scudiero, R.H. Shoemaker, K.D. Paull, et al. Evaluation of a soluble tetrazolium/formazan assay for cell growth and drug sensitivity in culture using human and other tumor cell lines. *Cancer Research*, 1988, 48(17): 4827−4833.

[22] M.V. Berridge, P.M. Herst, A.S. Tan. Tetrazolium dyes as tools in cell biology: New insights into their cellular r eduction. *Biotechnology Annual Review*, 2005, 11: 127−152. https://doi.org/10.1016/S1387-2656(05)11004-7

[23] A. De Logu, P. Uda, M.L. Pellerano, et al. Comparison of two rapid colorimetric methods for determining resistance of mycobacterium tuberculosis to rifampin, isoniazid, and streptomycin in liquid medium. *European Journal of Clinical Microbiology and Infectious Diseases*, 2001, 20(1): 33−39. https://doi.org/10.1007/PL00011234

[24] T.P. Wolter, D. von Heimburg, I. Stoffels, et al. Cryopreservation of mature human adipocytes. *Annals of Plastic Surgery*, 2005, 55(4): 408−413. https://doi.org/10.1097/01.sap.0000181345.56084.7d

[25] G. Strotel, A. Bokhof, J.C.W. Comley. Viability of *Onchocerca volvulus in vitro*. *Parasitology*, 1993, 107(2): 175–182. https://doi.org/10.1017/S0031182000067287

[26] T.M. Buttke, J.A. McCubrey, T.C. Owen. Use of an aqueous soluble tetrazolium/formazan assay to measure viability and proliferation of lymphokine-dependent cell lines. *Journal of Immunological Methods*, 1993, 157(1/2): 233–240. https://doi.org/10.1016/0022-1759(93)90092-L

[27] A.M. Kołodziejczyk, M.M. Grala, A. Zimon, et al. Investigation of HUVEC response to exposure to PAMAM dendrimers: Changes in cell elasticity and vesicles release. *Nanotoxicology*, 2022, 16(3): 375−392. https://doi.org/10.1080/17435390.2022.2097138

[28] H.D. Ratcliffe, J.W. Drozd, A.T. Bull. The utilization of l-glutamine and the products of its thermal decomposition by Klebsiella pneumoniae and Rhizobium leguminosarum. *FEMS Microbiology Letters*, 1978, 3(2): 65−69. https://doi.org/10.1111/j.1574-6968.1978.tb01885.x

[29] S. Kamineni, C.F. Huang. The antibacterial effect of sonication and its potential medical application. *SICOT-J*, 2019, 5: 19. https://doi.org/10.1051/sicotj/2019017

[30] A. Birmpa, V. Sfika, A. Vantarakis. Ultraviolet light and ultrasound as non-thermal treatments for the inactivation of microorganisms in fresh ready-to-eat foods. *International Journal of Food Microbiology*, 2013, 167(1): 96−102. https://doi.org/10.1016/j.ijfoodmicro.2013.06.005